Phase errors elimination in compact digital holoscope (CDH) based on a reasonable mathematical model

Yongfu Wen*[a], Weijuan Qu[a], Cheeyuen Cheng[a], Zhaomin Wang[a,b], Asundi Anand[b]
[a]Centre for Applied Photonics and Laser Technology, Ngee Ann Polytechnic, 535 Clementi Road, Singapore 599489; [b]Centre for Optical and Laser Engineering, School of Mechanical and Aerospace Engineering, Nanyang Technological University, Nanyang Avenue, Singapore 639798

ABSTRACT

In the compact digital holoscope (CDH) measurement process, theoretically, we need to ensure the distances between the reference wave and object wave to the hologram plane exactly match. However, it is not easy to realize in practice due to the human factors. This can lead to a phase error in the reconstruction result. In this paper, the strict theoretical analysis of the wavefront interference is performed to demonstrate the mathematical model of the phase error and then a phase errors elimination method is proposed based on the advanced mathematical model, which has a more explicit physical meaning. Experiments are carried out to verify the performance of the presented method and the results indicate that it is effective and allows the operator can make operation more flexible.

Keywords: Digital holography, phase error, holographic interferometry, surface fitting.

1. INTRODUCTION

In recent years, digital holography (DH) has been demonstrated to be a powerful technique in measuring microscopic samples. The basic advantage of DH is particularly useful for acquiring the intensity and phase of a specimen from a single hologram. This method is suitable for the testing of cells, semiconductor wafers and other micro-systems samples, with full-field and real-time features, for static and dynamic inspections[1-3]. *P. Ferraro et al*[4] applied the digital holography as an interferometric tool for measuring the out-of-plane deformation of Micro-electro-mechanical structures. *Dierter et al*[5] investigated the heart valve bio-prostheses with a setup for lens-less Fourier holography. *C. Yuan et al*[6] reported a lens-less digital holography system with short-coherence light source for recording 3D surface contouring of reflecting micro-objects. *V.R. Singhetal*[7] investigated the dynamic characterization of a MEMS diaphragm using lens-less time-averaged in-line reflection digital holography. Later, they developed a commercial handheld reflective digital holography system, compact digital holoscope (CDH), which can be incorporated with the device fabrication tools to monitor the process parameters[8].

Theoretically, in CDH (see Fig.1), the reference wave and object wave needs to match strictly on the hologram plane. In other words, we must accurately adjust the distance between the point source of reference wave to the hologram plane to be equal to the distance between the point sources of object wave to the hologram plane[9], by either controlling the position of the reference mirror or by controlling the position of the specimen with high precision motion stages. However, it is not easy to ensure that the two distances are strictly equal in practice, which will produce a misadjustment error. Then it will introduce a phase error during the reconstruction process and cause a serious phase distortion in the reconstructed phase map. At present, many researchers focus on the compensation of the residual quadratic phase factor caused by the microscope objective (MO) in the digital holographic microscopy (DHM), such as *Cuche et al* described a numerical method using a single hologram, of which four reconstruction parameters need to be iteratively adjusted[10]. A two dimensional fitting method with Zernike polynomials is presented by *Miccio et al*[11] to correct the quadratic curvature. *Zhou et al*[12] presented a phase subtraction method to compensate accurately the system phase aberration, but the method should capture two holograms to eliminate the phase aberration, which is not suitable for dynamic measurement.

In this paper, we focus on the elimination of phase errors caused by the misadjustment errors in CDH. Firstly, the strict theoretical analysis of the wavefront interference is performed to demonstrate the mathematical model of the phase error and then a phase errors elimination method is proposed based on the advanced mathematical model, which has a more explicit physical meaning. The proposed method will reduce the dependence on the high precision motion stages and will make the operation more flexible. This paper can be structured as follows. In Section 2, the basic theory of CDH

*wyf_optics@yahoo.com; phone +65 6460 6358

International Conference on Experimental Mechanics 2014, edited by Chenggen Quan, Kemao Qian, Anand Asundi, Fook Siong Chau, Proc. of SPIE Vol. 9302, 930207

is described and then a strict theoretical analysis of the wavefront interference between the reference wave and object wave is performed. Based on the theory analysis result, a new and advanced mathematical model is established to fit the unwrapped phase to remove the unwanted phase error. In Section 3, experiments are carried out to verify the performance of the proposed method. Finally the conclusion and discussion are given in Section 4.

2. BASIC THEORY

2.1 The principle of compact digital holoscope (CDH)

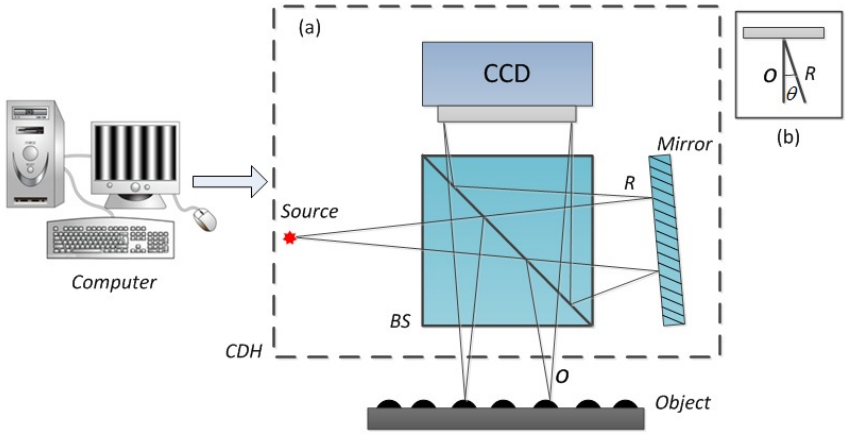

Figure 1. (a) Configuration of CDH; (b) the detail of the off-axis geometry.

The CDH system is built up by the Michelson interferometer configuration, as shown in Fig.1(a). A point light source provides a diverging beam and a cube beam splitter is used to separate the diverging beam into two portions. The scattered light from the tested object is called object wave, and the reflection beam from the mirror is the reference wave. The two waves produce interference in the CCD plane (hologram plane), the interference pattern is called digital hologram. The interference angle as shown in Fig.1(b) can be controlled by tilting the reference mirror, and this can be used in the system in off-axis mode.

In the hologram plane, the intensity image $I(x,y)$ of the recorded hologram can be written as

$$I(x,y) = |O+R|^2 = |O|^2 + |R|^2 + R^*O + RO^* \tag{1}$$

where $R(x,y)$ and $O(x,y)$ are the reference wave and object wave, respectively; $|O|^2 + |R|^2$, R^*O and RO^* are the DC term, the virtual term and the real term, respectively. * denotes the complex conjugate. In the CDH configuration, the three terms are well separated by filtering in the two-dimensional Fourier spectrum[13]. The spectrum $\psi_H^F(x,y)$ of the virtual image term R^*O can be extracted and then can be propagated to image plane to get a focused image $\psi^I(x,y)$. There are two main numerical reconstruction algorithms to describe the relationship of propagation between $\psi_H^F(x,y)$ and $\psi^I(x,y)$: the single Fresnel transform formulation and the angular spectrum method [14]. In this paper, the angular spectrum method is carried out to obtain the reconstructed wavefront[15] as follows

$$\begin{cases} \psi^I(n\Delta x_I, m\Delta y_I) = \dfrac{\exp(jkd)}{j\lambda d} IFFT\{FFT[\psi^H(n\Delta x_H, m\Delta y_H)] \times h(n\Delta\xi, m\Delta\eta)\} \\ h(n\Delta\xi, m\Delta\eta) = \exp[j\dfrac{2\pi d}{\lambda}\sqrt{1-(\lambda n\Delta\xi)^2-(\lambda m\Delta\eta)^2}] \end{cases} \tag{2}$$

where $h(n\Delta\xi, m\Delta\eta)$ is the optical transfer function in the spatial frequency domain, n and m are integers($-M/2 \le n \le M/2, -N/2 \le m \le N/2$, and $M \times N$ is the number of pixels of the CCD). $\Delta\xi$ and $\Delta\eta$, Δx_H and

Δy_H , Δx_I and Δy_I are sampling intervals in the spatial frequency domain, the hologram plane and the image plane, respectively. Then the intensity image and the phase map of the reconstruction image can be expressed as

$$\begin{cases} I^I(n\Delta x_I, m\Delta y_I) = \left|\psi^I(n\Delta x_I, m\Delta y_I)\right|^2 \\ \phi^I(n\Delta x_I, m\Delta y_I) = \arctan\{\dfrac{\mathrm{Im}[\psi^I(n\Delta x_I, m\Delta y_I)]}{\mathrm{Re}[\psi^I(n\Delta x_I, m\Delta y_I)]}\} \end{cases} \tag{3}$$

It should be noted that the phase map obtained by Eq.(3) is wrapped. To get the real phase of object $\Phi(n\Delta x_I, m\Delta y_I)$, the well-known phase unwrapping algorithms can be used.

2.2 Theoretical analysis and mathematic model establishment

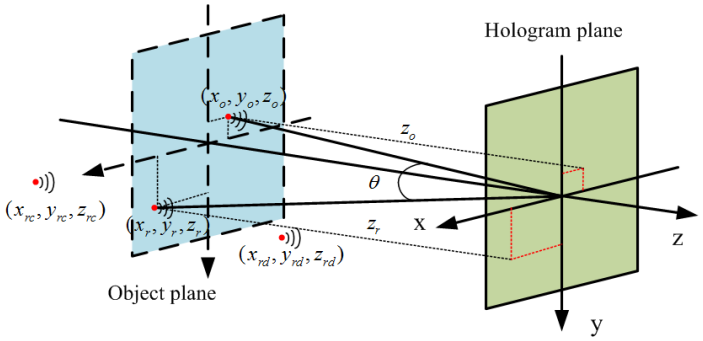

Figure 2. Sketch map of the location of the two point sources.

The geometry of the reconstruction algorithm is illustrated in the above section. Here let us assume that the reference wave is generated by a point source, which located at (x_r, y_r, z_r) and the object wave is also generated by a point source, which located at (x_o, y_o, z_o), where z_o and z_r are the distances between the point sources of the reference wave and object wave to the recombining location of the two beams, as shown in Fig.2. Then, the reference wave and object wave in the holography plane can be expressed as follows [16]

$$R(x,y) = \exp\{-\frac{jk}{2z_r}[(x-x_r)^2 + (y-y_r)^2]\} \tag{4}$$

$$O(x,y) = A_0 \exp\{-\frac{jk}{2z_o}[(x-x_o)^2 + (y-y_o)^2]\}\exp[j\varphi_{object}(x,y)] \tag{5}$$

where $\varphi_{object}(x,y)$ and A_0 are the phase of object tested and the amplitude, respectively. By geometric deduction, the corresponding intensity image can be rewritten as follows

$$\begin{aligned} I(x,y) &= (|O|^2 + |R|^2) + R^*O + RO^* \\ &= (1 + A_0^2) \\ &+ A_0 \exp[j\varphi_{object}(x,y)]\times \\ &\exp\{\frac{jk}{2}(\frac{1}{z_o} - \frac{1}{z_r})(x^2+y^2) - jk(\frac{x_o}{z_o} - \frac{x_r}{z_r})x - jk(\frac{y_o}{z_o} - \frac{y_r}{z_r})y + [\frac{jk}{2z_o}(x_o^2 + y_o^2) - \frac{jk}{2z_r}(x_r^2 + y_r^2)]\} \\ &+ A_0 \exp[-j\varphi_{object}(x,y)]\times \\ &\exp\{-\frac{jk}{2}(\frac{1}{z_o} - \frac{1}{z_r})(x^2+y^2) + jk(\frac{x_o}{z_o} - \frac{x_r}{z_r})x + jk(\frac{y_o}{z_o} - \frac{y_r}{z_r})y + [-\frac{jk}{2z_o}(x_o^2 + y_o^2) + \frac{jk}{2z_r}(x_r^2 + y_r^2)]\} \end{aligned} \tag{6}$$

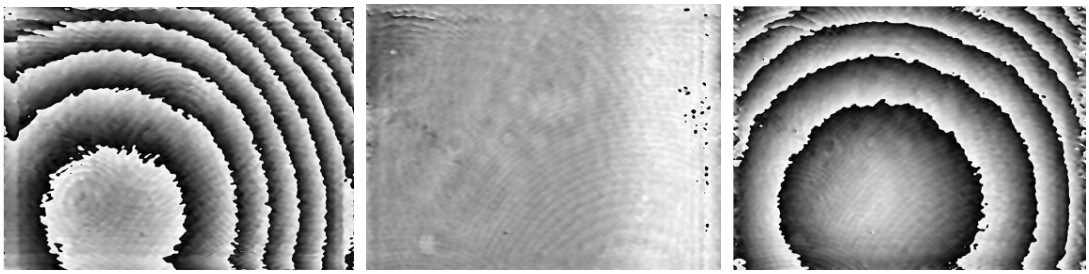

(a) (b) (c)

Figure 3. Reconstruction phase for the changing of the positions: (a) when $z_o > z_r$, there is a converging quadratic with X and Y direction tilt; (b) when $z_o = z_r$, there is a quasi-flat phase;(c) when $z_o < z_r$, there is a diverging quadratic wave with x and y tilt.

According to Eq.(6), the virtual image term R^*O combines not only the phase of object but also four phase error terms which include two linear terms (off-axis tilts), a quadratic term and a constant phase term. A close inspection of Eq.(6) and Fig.3 reveals that the quadratic phase term is generated by $z_o \neq z_r$. For example, the reference point source located at (x_{rc}, y_{rc}, z_{rc}) or (x_{rd}, y_{rd}, z_{rd}) in Fig.2, and its corresponding reconstruction phase map is Fig.3(a) or Fig.3(c). If we can precisely adjust $z_o = z_r$ in the measurement process, the quadratic phase term will disappear, such as Fig.3(b). Actually, z_o and z_r are not easy to measure and quantify in the experiment. In addition, in order to remove the off-axis tilts, we can orientate the maximum value of frequency spectrum domain, which is an easy way to remove the tilts. However, the phase curvature is difficult to be completely eliminated, which makes the spectrum centering difficult due to the fluctuating boundary. Thus the phase reconstructed from the hologram can be written as

$$\Phi_{rec}(x,y) = \varphi_{object}(x,y) + \varphi_{error}(x,y) \tag{7}$$

where $\Phi_{rec}(x,y)$ is the unwrapping phase of the holographic reconstruction, $\varphi_{object}(x,y)$ is the ideal phase of the object tested, $\varphi_{error}(x,y)$ is the phase errors map. In CDH, the phase of object $\varphi_{object}(x,y)$ is usually very small and varies quickly. Therefore, it can be regarded as a weak perturbation on the phase error[17,18]. Based on the analysis above, the phase error $\varphi_{error}(x,y)$ can be acquired by the fitting algorithm based on the proposed advanced mathematical compensation model as follows

$$\phi_{error}(x,y) = a(x^2 + y^2) + bx + cy + d \tag{8}$$

where, a, b, c, d are the coefficients of quadratic term, tilt terms in the x and y direction, the constant term, respectively. It can clearly be seen that the mathematical compensation model of Eq.(8) is in accordance with the phase error terms of Eq.(6). It is demonstrated that the model has a more explicit physical meaning than the simple spherical equation[17] and XY polynomial[18]. To solve Eq.(8) for the unknown coefficients, the least squares (LS) method normally can be used. Because the LS fitting process minimizes the summed square of the residuals, the coefficients are determined by differentiating L with respect to each parameter, and setting the result equal to zero, see as Eq.(9) and Eq.(10). If the number of sampling point K is greater than the number of unknowns, then the system of equations is over-determined.

$$L = \sum_{i=1}^{K} \left\{ \Phi^i_{rec} - \left[a(x_i^2 + y_i^2) + bx_i + cy_i + d \right] \right\}^2 \rightarrow \min \tag{9}$$

$$\begin{cases} \dfrac{\partial L}{\partial a} = -2\sum_{i=1}^{K}[\Phi_{rec} - a(x_i^2 + y_i^2) - bx_i - cy_i - d](x_i^2 + y_i^2) = 0 \\ \dfrac{\partial L}{\partial b} = -2\sum_{i=1}^{K}[\Phi_{rec} - a(x_i^2 + y_i^2) - bx_i - cy_i - d]x_i = 0 \\ \dfrac{\partial L}{\partial c} = -2\sum_{i=1}^{K}[\Phi_{rec} - a(x_i^2 + y_i^2) - bx_i - cy_i - d]y_i = 0 \\ \dfrac{\partial L}{\partial d} = -2\sum_{i=1}^{K}[\Phi_{rec} - a(x_i^2 + y_i^2) - bx_i - cy_i - d] = 0 \end{cases} \tag{10}$$

Finally, we can obtain the matrix equation as Eq.(11).

$$\begin{bmatrix} a \\ b \\ c \\ d \end{bmatrix} = \begin{bmatrix} \sum (x_i^2 + y_i^2)^2 & \sum x_i(x_i^2 + y_i^2) & \sum y_i(x_i^2 + y_i^2) & \sum (x_i^2 + y_i^2) \\ \sum x_i(x_i^2 + y_i^2) & \sum x_i^2 & \sum x_i y_i & \sum x_i \\ \sum y_i(x_i^2 + y_i^2) & \sum x_i y_i & \sum y_i^2 & \sum y_i \\ \sum (x_i^2 + y_i^2) & \sum x_i & \sum y_i & K \end{bmatrix}^{-1} \begin{bmatrix} \sum (x_i^2 + y_i^2)\Phi_{rec} \\ \sum x_i \Phi_{rec} \\ \sum y_i \Phi_{rec} \\ \sum \Phi_{rec} \end{bmatrix} \tag{11}$$

After calculating these coefficients by Eq.(11), we can obtain the real object phase $\varphi_{object}(x, y)$ by removing the unwanted phase error $\varphi_{error}(x, y)$ from the reconstruction phase $\Phi_{rec}(x, y)$.

3. EXPERIMENTAL VERIFICATION

To verify the validity of the proposed method, some experiments were carried out. The setup of the CDH is shown in Fig.4. The light emitted from a 633nm He-Ne laser is coupled to a single mode fiber as a point light source. The compact CDH is fixed on a XYZ motion platform. The digital hologram is recorded by a CCD camera with pixel resolution is 1280×960 and pixel size is 4.65μm×4.65μm. Figure 5(a) shows the digital hologram captured by the setup of Fig.4, when $z_o < z_r$. Fig.5(b) is the intensity distribution of wafer tested. Fig.5(c) and Fig.5(d) show the reconstructed wrapped and unwrapping phase map of wafer directly extracted from Fig.5(a) with the angular spectrum algorithm respectively. It is noteworthy that the spherical curved and tilt phase errors introduced by the adjustment errors[19] are clearly seen in the whole field of view, which is similar to Fig.3(c).

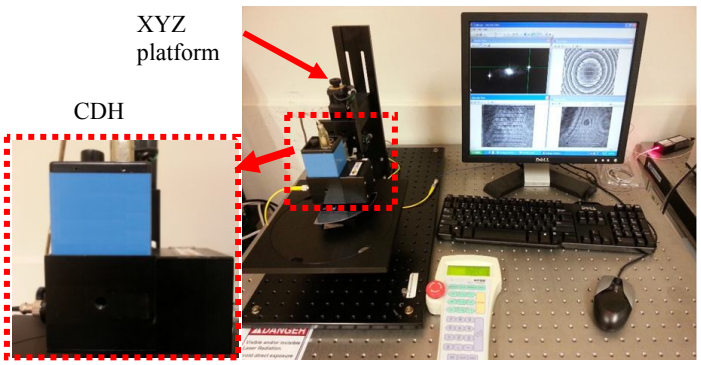

Figure 4. The setup of the CDH with XYZ motion platform.

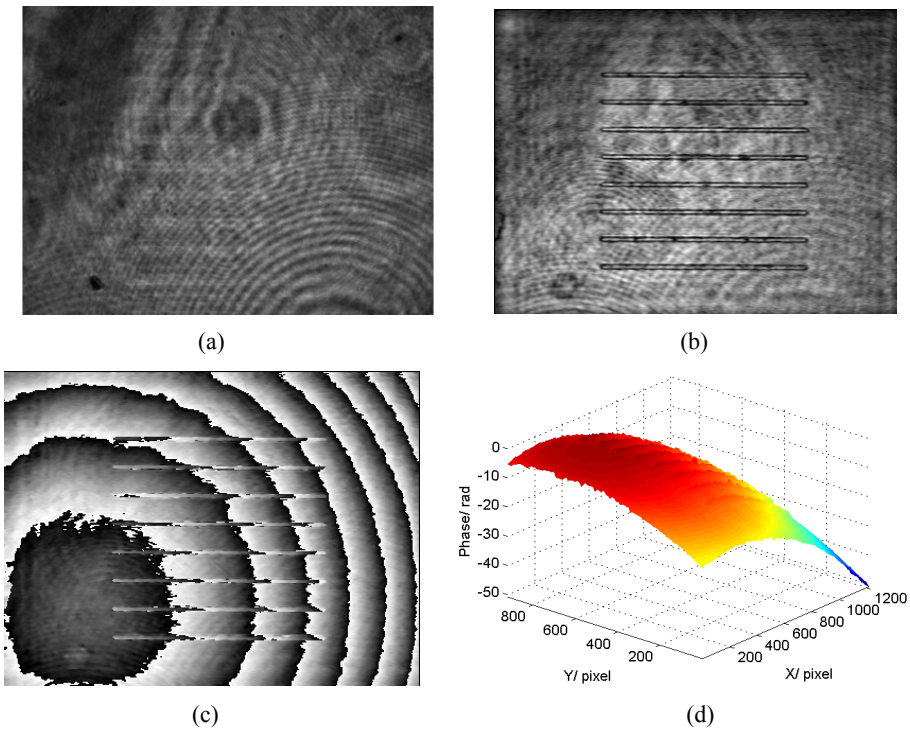

Figure 5. The experimental result by CDH: (a) the digital hologram of the wafer; (b) the intensity image; (c) wrapped phase reconstructed; (d) unwrapping phase reconstructed.

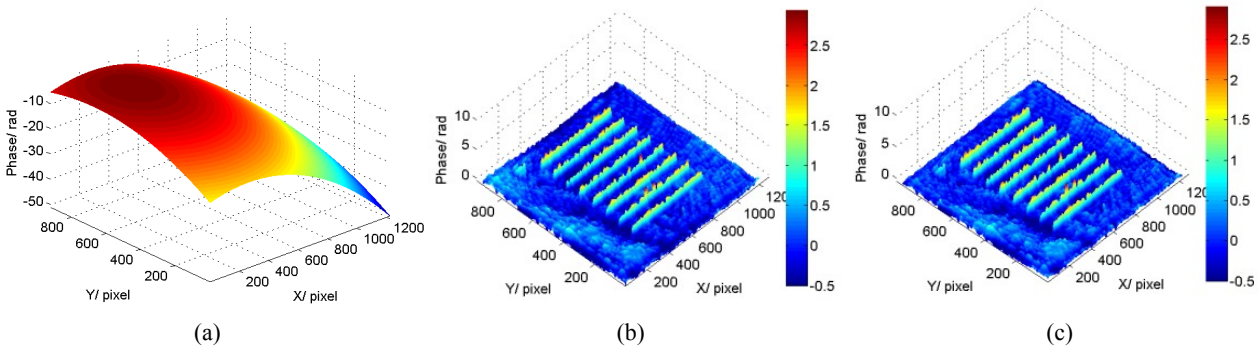

Figure 6. Results: (a)fitted aberration; the correct phase map by (b) proposed method; (c) Zernike fitting method.

Fig.6(a) shows the fitting phase error term $\varphi_{error}(x,y)$ of Fig.5(d) with the proposed method. Fig.6(b) gives the phase corrected by subtracting Fig.6(a) from Fig.5(d). It is shown that the feature of the wafer is clearly seen within the whole field of view. To further verify the validity of the proposed method, the Zernike fitting method[20] is introduced to compare with our method. Fig.6(c) shows the phase corrected by Zernike method. It demonstrates that the two recovered phase maps look similar to each other. However, in this experiment, 1228800 (1280×960) sampling points are chosen from the original phase matrix and the processing time of the two methods are 0.22s (proposed method) and 5.94s (Zernike fitting with 21 polynomials), respectively, with 2.67 GHz Core (TM) i7 CPU using MATLAB 7.11.

A wafer used for the microphone is selected as another specimen to further indicate the proposed method. Fig.7(a) is the hologram of the wafer, when $z_o > z_r$, and its intensity image is given in Fig.7(b). The wrapped phase reconstructed and unwrapped phase reconstructed are given in Fig.7(c) and Fig.7(d), respectively. Fig.7(e) shows the fitting phase error term $\varphi_{error}(x,y)$ of Fig.7(d). Fig.7(f) displays the phase map corrected of specimen by proposed method.

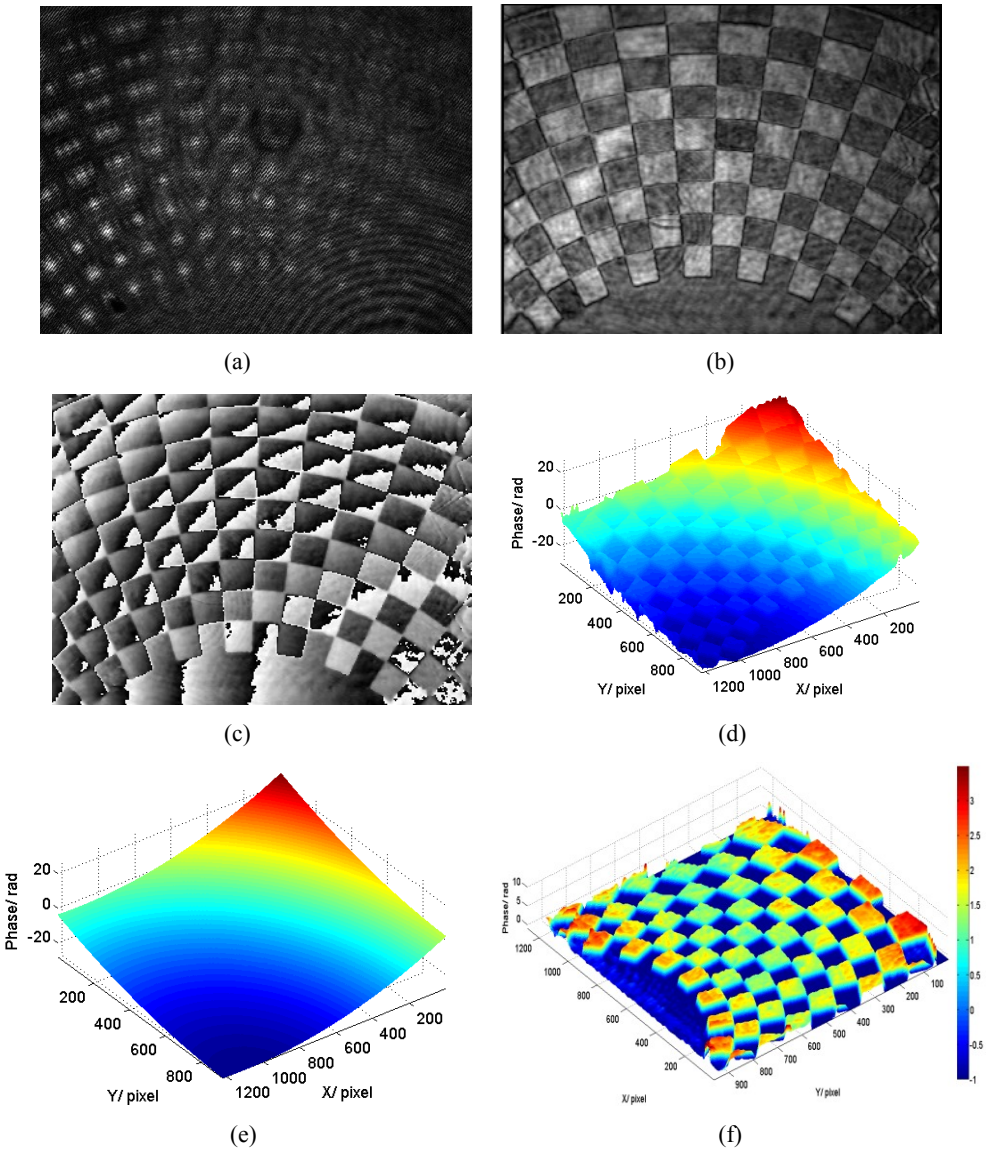

Figure 7. The experimental results with CDH: the hologram (a) and the intensity (b) of the wafer; (c) the wrapped phase reconstructed; (d) unwrapping phase map; (e) the fitting error curvature;(f) the phase map corrected by proposed method.

4. CONCLUSIONS AND DISCUSSION

In this paper, we focus on the elimination of phase errors caused by the misadjustment errors ($z_o \neq z_r$) in CDH. Firstly, the strict theoretical analysis of the wavefront interference is performed to demonstrate the mathematical model of the phase error and then a phase error elimination method is proposed based on the advanced mathematical model, which has a more explicit physical meaning. The experiment results acquired show that the proposed method is quite useful and simple in CDH system. Moreover, it allows the operation of the CDH system without a precision motion stage, which can be freely adjusted.

Note that, for the phase compensation method [13,17,18,20], the phase data of specimen is usually very small and varies quickly and can be regarded as a weak perturbation on the phase errors. However, these phase compensation methods will be failure (see Fig.8), when the phase data of specimen is big enough. It is clearly seen from Fig.8 that there is an obvious quadratic error in Fig.8(b) and Fig.8(c). To overcome this case, we can select some sampling points without specimen information on the specimen areas to fit the phase errors[20]. Fig.9(a) shows the sampling points extracted from

Fig.8(a) without specimen information. After removing the fitting phase error, we can get the compensation results, as shown in Fig.9(b) and Fig.9(c).

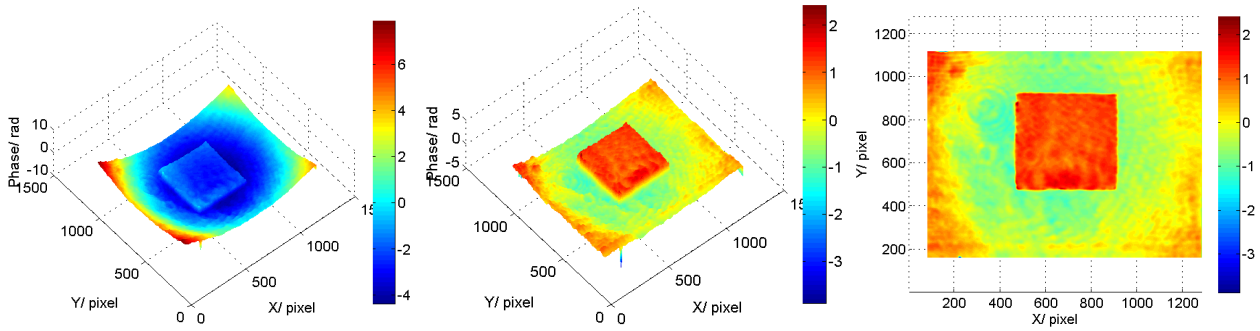

(a) (b) (c)

Figure 8. (a) the phase map of specimen with phase error; (b)3D map and (c) 2D map of compensation result.

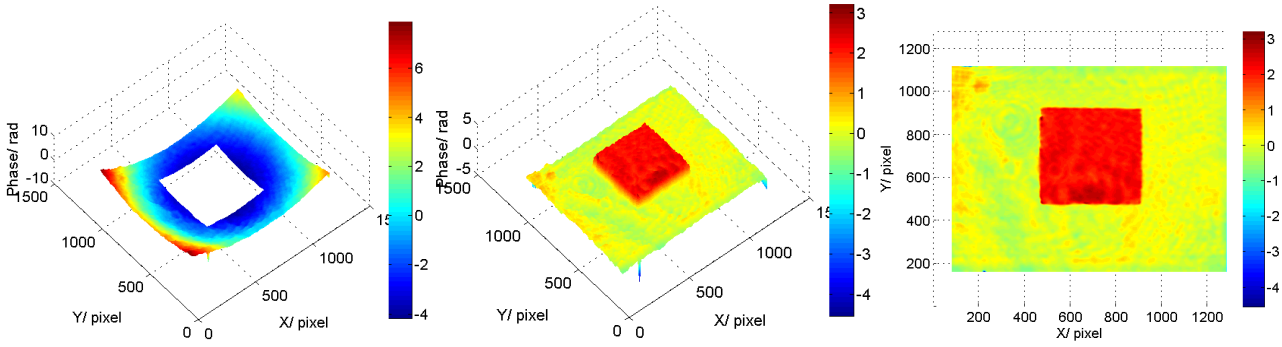

(a) (b) (c)

Figure 9. (a) sampling points extracted from Fig.8(a) without the specimen information; (b)3D map and (c) 2D map of compensation result.

Acknowledgement

This study is supported by Translational R&D and Innovation Fund (TIF) grants MOE2012-TIF-1-T-003 and MOE2013-TIF-2-G-012 from the Singapore Ministry of Education.

Reference

[1] Khmaladze, M. Kim, and C.M. Lo, "Phase imaging of cells by simultaneous dual-wavelength reflection digital holography," Opt. Express 16(15),10900-10911(2008).

[2] Y. Emery, E. Cuche, and F. Marquet, "Digital holographic Microscopy (DHM) for metrology and dynamic characterization of MEMS and MOEMS," Proc. SPIE 6186, 6186N-1(2006)

[3] L. Xu, X. Peng, J. Miao, and A.K. Asundi, "Studies of Digital Microscopic Holography with Applications to Microstructure Testing," Appl. Optics 40(28), 5046-5051(2001)

[4] P. Ferraro, S. D. Nicola, and G. Coppola, "Testing silicon MEMS structures subjected to thermal loading by digital holography," Proc. SPIE 5343, 235-243 (2004)

[5] Dieter Dirksen, H. Drostea, and B. Kemper, "Lensless Fourier holography for digital holographic interferometry on biological samples," Opt. Lasers Eng. 36(3), 241-249 (2001)

[6] C. Yuan, H. Zhai, and X. Wang, "Lensless digital holography with short-coherence light source for three-dimensional surface contouring of reflecting micro-object," Optics Commu.270(2),176-179(2007).

[7] V. R. Singh, J. Miao, and Z. Wang, "Dynamic characterization of MEMS diaphragm using time averaged in-line digital holography," Opt. Commu. 280(2), 285-290(2007)

[8] V. R. Singh, L. S. Sui, and A. Asundi, "Compact handheld digital holographic microscopy system development," Proc. SPIE 7522, 75224L-1(2010)

[9] W. Qu, O. Chee, and T. R. Lewis, "Physical spherical phase compensation in reflection digital holographic microscopy," Opt. Lasers Eng. 50(4), 563-567(2012)
[10] E. Cuche, P. Marquet, and C. Depeursinge, "Simultaneous amplitude-contrast and quantitative phase-contrast microscopy by numerical reconstruction of Fresnel off-axis holograms," Appl. Opt. 38(34), 6994-7001(1999)
[11] L. Miccio, D. Alfieri, and S. Grilli, "Direct full compensation of the aberrations in quantitative phase microscopy of thin objects by a single digital hologram," Appl. Phys. Lett. 90(4), 041104(2007)
[12] W. Zhou, Y. Yu, and A. Asundi, "Study on aberration suppressing methods in digital micro-holography," Opt. Lasers Eng. 47(2), 264-270(2009)
[13] C. Zuo, Q. Chen, W.J. Qu, and A. Asundi, "Phase aberration compensation in digital holographic microscopy based on principal component analysis," Opt. Lett. 38(10), 1724-1726(2013)
[14] Ulf Schnars, and P. Werner, "Digital recording and numerical reconstruction of holograms,"Meas.Sci. Technol. 13(9), 85-101(2002)
[15] W. J. Qu, O. C. Chee, and Vijay R. S., "Quasi-physical phase compensation in digital holographic microscopy," J. Opt. Soc. Am. A26(9),2005-2011(2009)
[16] F. Montfort, F. Charrière, and T. Colomb, "Purely numerical compensation for microscope objective phase curvature in digital holographic microscopy: influence of digital phase mask position," J. Opt. Soc. Am. A 23(11), 2944-2953(2006)
[17] J. L. Di, J. L. Zhao, and W. W. Sun, "Phase aberration compensation of digital holographic microscopy based on least squares surface fitting," Opt. Commun. 282(19), 3873-3877(2009)
[18] Y. Z. Zhang, D. Y. Wang, and Y. X. Wang, "Automatic Compensation of Total Phase Aberrations in Digital Holographic Biological Imaging," Chin. Phys. Lett. 28(11), 114-209(2011)
[19] W. J. Qu, O. C. Chee, Y. J. Yu, and A. Asundi, "Microlens characterization by digital holographic microscopy with physical spherical phase compensation," Appl. Opt. 49(33), 6448-6454(2010)
[20] T. Colomb, F. Montfort, and J. Kühn, "Numerical parametric lens for shifting, magnification, and complete aberration compensation in digital holographic microscopy," J. Opt. Soc. Am. A 23(12), 3177-3190 (2006)